Variance-ranked sound speed bases misclassify the surface duct: limits of profile RMSE as a proxy for acoustic prediction skill in the Bay of Bengal

Derin George
Thalwag · Kochi, India
Indian Maritime University · Visakhapatnam, India
derin@thalwag.com
ORCID 0009-0006-2965-9222

Preprint · not peer-reviewed · September 16, 2026

Abstract

Sound speed profile (SSP) estimation from surface observables is operationally mature and is evaluated almost universally by profile root-mean-square error. Using 19 934 Argo profiles from the Bay of Bengal (2005–2020), season-stratified empirical orthogonal function (EOF) bases, and BELLHOP transmission loss (TL) at 500 Hz, 1500 Hz and 3500 Hz over 24 held-out locations, we show that this metric can be decoupled from, and even inverted relative to, acoustic prediction skill. The mechanism is a property of the basis. A variance-ranked EOF expansion places its leading modes at the depth of maximum variance, near 100 m, whereas surface-duct trapping is decided in the upper 60 m. Supplied with *exact* coefficients, a four-mode reconstruction attains an RMS error of $0.906\,\mathrm{m\,s^{-1}}$ - 4.4 times smaller than climatology - yet classifies duct trapping correctly in only 75.3 % of held-out profiles, below climatology's 76.3 %. Twelve modes reach 91.6 %. The additional modes carry 4.4 % of the variance and are recovered from perfect surface observables at mean $R^2 = 0.10$, leaving a 13.3 percentage-point observability gap. A pre-registered intervention, re-weighting the training objective toward the duct, reduced profile RMSE further but did not improve acoustic error: the criterion required 1.5 dB and the outcome was -3.97 dB with a 95 % upper bound of $+0.86$ dB. Replacing idealised dynamic height with DUACS altimetry degrades RMSE from 2.124 to $2.923\,\mathrm{m\,s^{-1}}$ while changing duct classification by 0.9 points. We conclude that SSP products intended for acoustic use should be evaluated acoustically, and that in this basin the accuracy the acoustics requires is not attainable from the surface.

Keywords: sound speed profile; empirical orthogonal functions; surface duct; transmission loss; satellite altimetry; Bay of Bengal

1 Introduction

Electromagnetic radiation is absorbed within metres in seawater, so sound is the only long-range information carrier in the ocean interior. Every underwater acoustic prediction - sonar detection range, communication link budget, tomographic inversion, marine mammal exposure - depends on the sound speed field, and that field is sampled far more sparsely than it varies.

The standard response is to infer the subsurface from the surface. Carnes and colleagues established the modern form of this approach: project historical profiles onto empirical orthogonal functions and regress the leading coefficients on satellite sea surface temperature and sea surface height [Carnes et al.(1990), Fox et al.(2002)]. The method is operational in the U.S. Navy's Modular Ocean Data Assimilation System and has been extended with tree ensembles [Ou et al.(2022)], recurrent networks [Li et al.(2024)], three-dimensional convolutional models [Li et al.(2025)], and residual correction schemes [Yang et al.(2026)].

These studies are evaluated, with few exceptions, by profile RMS error. The implicit assumption is that a profile closer in RMS produces acoustics closer in decibels. Where acoustic validation is performed it is generally confirmatory: Li et al. [Li et al.(2024)] report that the model with lower SSP RMSE also produced lower TL RMSE, and Yang et al. [Yang et al.(2026)] report a reduction in TL mean absolute error accompanying a reduction in field RMSE. The same study [Yang et al.(2026)] also notes, in passing, that one of their climatological baselines achieved a lower mean TL error than a learned model, with a bootstrap interval crossing zero. That observation is not developed.

The assumption deserves scrutiny because the physics is not obviously compatible with it. RMS error is an integral over depth weighted by nothing in particular. Acoustic propagation in shallow water is controlled by whether a near-surface sound speed maximum exists, where it sits relative to the source, and whether the frequency exceeds the duct cutoff. Those are threshold properties of a thin layer. An error metric that averages over 200 m of water column has no particular reason to track them.

We test this directly in the Bay of Bengal, chosen because it is acoustically difficult and thinly studied. Monsoonal freshwater discharge caps the basin with a low-salinity layer, producing barrier layers and temperature inversions that decouple the sound speed structure from surface temperature. This paper makes four contributions.

1. We show that variance-ranked EOF truncation, at the order an RMSE criterion selects, misclassifies surface-duct trapping *even when supplied with exact coefficients*, and does so worse than climatology (Section 4.3).

2. We show that reducing profile RMSE by 47 % buys only a 12 % to 17 % reduction in acoustic error, and that an objective re-weighted toward the duct reduces RMSE further while failing a pre-registered acoustic criterion (Sections 4.4 and 4.5).

3. We separate a representation limit from an observability limit by means of an oracle experiment, and quantify the gap (Section 4.3).

4. We quantify the cost of replacing idealised dynamic height with real gridded altimetry (Section 4.6).

Where we describe a result as new, we mean to our knowledge; the literature in this area is large and actively growing.

2 Data

2.1 Profiles

Delayed-mode Argo temperature and salinity profiles were obtained for the region 80° to 95°E, 5° to 22°N. Profiles were retained if they contained at least ten good levels, reached shallower than 15 m, extended below 200 m, and yielded sound speeds between 1400 and 1600 m s^{-1}. Each profile was interpolated onto a common 5 m grid, and sound speed computed with the TEOS-10 equation of state via the `gsw` toolbox, using absolute salinity and conservative temperature.

Training used 2005–2018 (18 673 profiles after quality control and completeness to 480 m); testing used December 2019 to November 2020 (1261 profiles), held out entirely. The split is temporal, so no test-year information enters the basis or the regression.

2.2 Climatology

World Ocean Atlas 2023 monthly climatology at 1° resolution was interpolated to each profile position and month. Using the matching month matters: comparing a July profile against an annual mean would produce an artificially weak baseline. Over the held-out set the climatological sound speed error is 3.981 m s^{-1} RMS over 0 m to 200 m (n = 1278), with a bias of 0.727 m s^{-1}. Computed year by year over 2005–2020 the mean of the annual RMS values is 3.72(38) m s^{-1}, showing that the baseline is stable and that 2019–2020 is not anomalous.

2.3 Altimetry

Gridded sea level was taken from the Copernicus Marine multi-year product `SEALEVEL_GLO_PHY_L4_MY_008_047` (DUACS DT-2024, 0.125°, daily), variables `sla` and `adt`, collocated to each profile's position and *day* by linear interpolation. Matching to the day rather than the month is essential: the component of sea level that carries thermocline information is mesoscale, with eddy lifetimes of 30 d to 90 d. All 19 934 profiles matched. As an independent check on the files, the annual median sea level anomaly over the matched set rises at 4.17 mm yr^{-1}, consistent with the known regional rate.

3 Methods

3.1 Basis and estimator

Profiles were grouped into four seasons (winter DJF, pre-monsoon MAM, monsoon JJA, post-monsoon SON). Within each season the training profiles were centred on the seasonal mean and decomposed by singular value decomposition. The leading mode carries 69.5 % to 79.6 % of the variance depending on season; modes 5–12 together carry 4.4 %.

Coefficients were predicted from seven surface predictors - latitude, longitude, sin and cos of day-of-year, sea surface temperature, sea surface salinity, and a height term - using a random forest (150 trees, minimum leaf size 5) and, for comparison, ridge regression. Without a height term, linear ridge regression slightly outperforms the random forest (4.082 vs. 4.364 m s^{-1} RMS), but with dynamic height the forest attains greater skill (2.124 vs. 2.303 m s^{-1}), demonstrating that non-linear modeling primarily benefits the height projection. The height term is either dynamic height computed from the profile's own temperature and salinity referenced to 480 m (the idealised case) or satellite `sla` or `adt` (the real case).

Throughout we compare against a nominal accuracy target of 2.389 m s^{-1}, defined before any estimator was built as a 40 % reduction on the climatological error of 3.981 m s^{-1}. Figure panels label this target "Gate 0", the internal designation of the threshold.

3.2 Duct definition

The sonic layer depth (SLD) is the depth of the first near-surface sound speed maximum. A source at depth z_s is trapped when three conditions hold simultaneously: an SLD exists; $z_s \leq$ SLD; and the frequency exceeds the duct cutoff

$$f_c = \frac{1.84 \times 10^5}{H^{3/2}}, \tag{1}$$

with H the duct thickness in metres and f_c in hertz. The third condition is frequently omitted and matters here: a 35 m duct is physically real but cannot trap 500 Hz, because its cutoff is 890 Hz. Duct classification accuracy below means the fraction of profiles for which a reconstruction and the true profile agree on whether the source is trapped.

3.3 Acoustic model

Transmission loss was computed with BELLHOP (Fortran, via `AcousticsToolbox.jl`) on a 200 m shelf with a silty-clay seabed representing the Ganges–Brahmaputra mud belt. Source and receiver both at 30 m; 50 range bins to 25 km. Because the domain is shallower than the profiles, *no extrapolation is used*: every model input is measured data. Twenty-seven locations were selected stratified by latitude band and season, with three worst-case profiles appended; twenty-four yielded complete transmission loss fields at all three frequencies and are used throughout. (The consequences of the worst-case augmentation are discussed in Section 4.4.)

BELLHOP returns no result for receivers in deep shadow; across the runs reported here 14 % to 16 % of receivers were affected. The rate is not uniform across variants - at 1500 Hz it was 11.8 % for climatology, 15.3 % for the RMSE-trained estimator and 18.2 % for the duct-weighted one, consistent with sharper near-surface structure casting deeper shadows. All comparisons are made on locations where every variant returned a value, so the sample is complete by construction, but the differing rates mean the retained locations are not a random subset and we note this as a limitation of the paired comparison in Section 4.5.

3.4 Metrics

BELLHOP was run in its default coherent mode, so the raw output is a point-sampled coherent field. We report three quantities:

point the raw coherent $|\Delta \mathrm{TL}|$ at the 10 km bin;

smoothed a three-bin running median of TL in decibels, then differenced - the metric on which the pre-registered criterion of Section 4.5 was evaluated;

energy intensity averaged over ±2 km and converted back to decibels.

The energy metric is primary, for two reasons. Physically, detection depends on received energy in a range window, whereas a median of logarithmic values has no corresponding interpretation. Empirically, the point-wise metric ranks the estimator *worse* than climatology at 500 Hz and 3500 Hz while ranking it better on energy (Table 4); a metric that inverts the ranking of a method unambiguously closer to truth is not measuring the ocean.

There is a bound behind this. Two eigenrays interfere with relative phase $2\pi f \Delta t$, and an error field $\delta c(z)$ perturbs their differential travel time. Requiring the differential path-averaged error to stay within a quarter cycle gives

$$\delta c \le \frac{c^2}{4fR}. \tag{2}$$

At $R = 10\,\mathrm{km}$ and $c = 1540\,\mathrm{m\,s^{-1}}$, this is $0.119\,\mathrm{m\,s^{-1}}$ at 500 Hz, $0.040\,\mathrm{m\,s^{-1}}$ at 1500 Hz and $0.017\,\mathrm{m\,s^{-1}}$ at 3500 Hz. The best estimator here delivers $2.1\,\mathrm{m\,s^{-1}}$, and the four-mode truncation floor is $0.950\,\mathrm{m\,s^{-1}}$. Coherent point-wise TL is therefore unpredictable in principle at every frequency considered, by one to two orders of magnitude.

4 Results

4.1 Structure of the climatological error

Figure 1 shows climatological sound speed error against depth. The error is not uniform: it peaks near 100 m at $5.5\,\mathrm{m\,s^{-1}}$ and falls to about $1.0\,\mathrm{m\,s^{-1}}$ at the surface. Decomposition shows the peak is overwhelmingly thermal. The right panel of Figure 1 shows the salinity share of the error against the 0.03 value assumed in the canonical sound speed expression [Munk and Wunsch(1979)]; in this basin salinity contributes substantially more near the surface, which is the monsoonal freshwater cap appearing in the acoustic field. The mechanism behind the peak at depth is thermocline displacement - a climatology averages profiles whose thermoclines sit at different depths, and the average has a thermocline that matches none of them. The annual thermocline depth over 2005–2020 ranges from 84 to 104 m, so the variance maximum and the error maximum coincide by construction.

This is consistent with reports from the South China Sea, where reconstruction error likewise peaks near 100 m [Ou et al.(2022)]. It is the starting point of this paper rather than a result: *the variance lives at 100 m, and everything that follows is a consequence of a basis built to minimise variance.*

4.2 What the basis represents

Figure 2 shows the leading EOF modes. Mode 1, carrying 69.5 % to 79.6 % of the variance depending on season, peaks near 110 m and is close to zero at the surface: it is a thermocline displacement mode. Figure 3 confirms this directly: mode 1 correlates with thermocline depth at $r = -0.61$, while modes 2–4 do not (-0.24, $+0.10$, -0.05).

The consequence is structural. A variance-ranked basis allocates its leading modes to the depth of greatest variance. In this basin that is 100 m. At 1500 Hz with a 30 m source, the acoustically decisive structure is the sign and magnitude of the near surface gradient in the upper 60 m. **The basis is optimal for the wrong depth**, and the criterion that selects its truncation order - RMS error - is the metric this paper examines.

4.3 Two ceilings: representation and observability

To separate a failure of the basis from a failure of the data we ran an *oracle* experiment. Held-out profiles were projected onto the season-stratified basis and reconstructed using their *true* coefficients - no estimator, no surface data, no prediction of any kind - at truncation orders $K = 4, 6, 8, 12$. The reconstruction was then scored on duct classification. This isolates what the basis can carry from what the surface can supply. Results are in Table 1 and Figure 4.

Three readings follow, and the first is the central result of this paper.

The basis alone can be worse than climatology. At $K = 4$ the oracle achieves an RMS error of $0.906\,\mathrm{m\,s^{-1}}$, 4.4 times smaller than climatology's $3.981\,\mathrm{m\,s^{-1}}$, while classifying the propagation regime correctly 75.3 % of the time against climatology's 76.3 %. A reconstruction handed the right

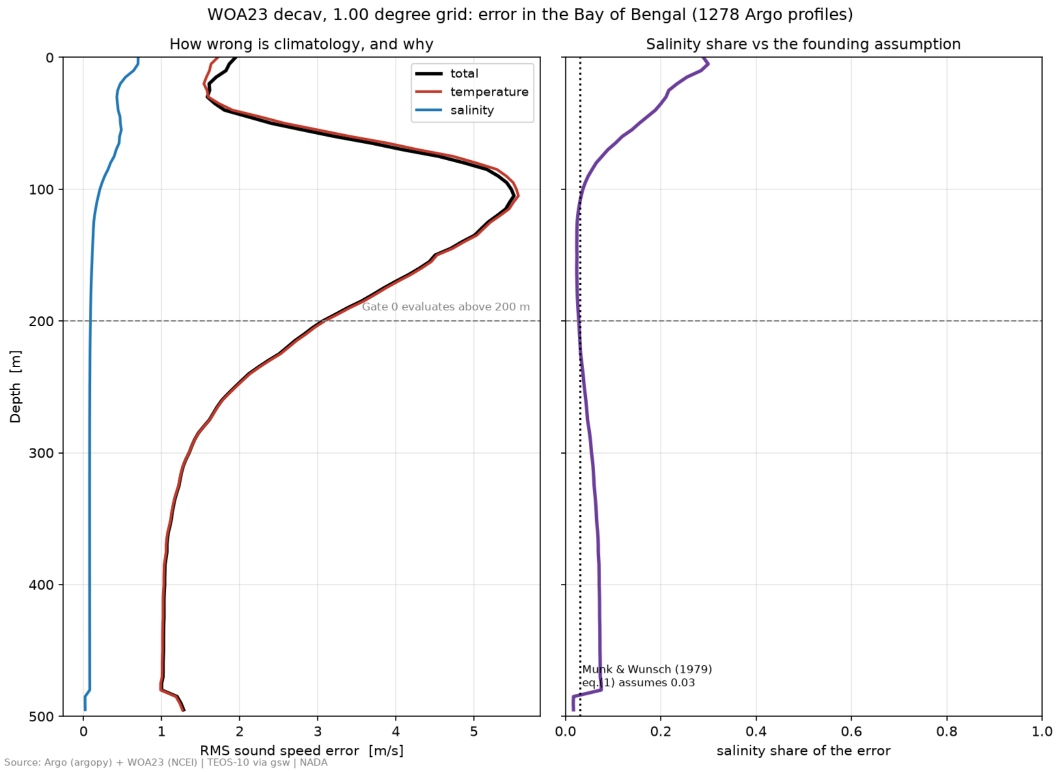

Figure 1: Climatological (WOA23) sound speed error against depth over the held-out set, with temperature and salinity contributions separated. The error peaks near 100 m and is smallest at the surface, where satellite observables are available.

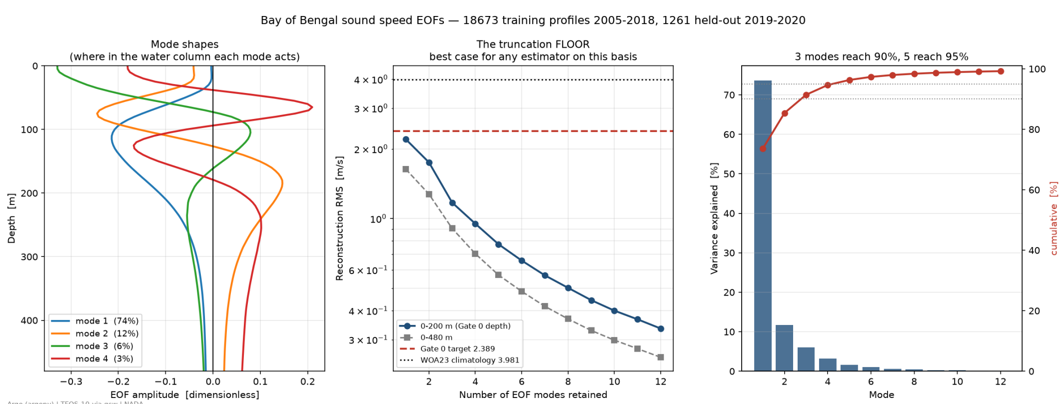

Figure 2: The season-stratified EOF basis. Mode 1 peaks near 110 m and is close to zero at the surface. (Note: the panel title quotes the global-basis variance share; seasonal shares are 69.5 % to 79.6 %.)

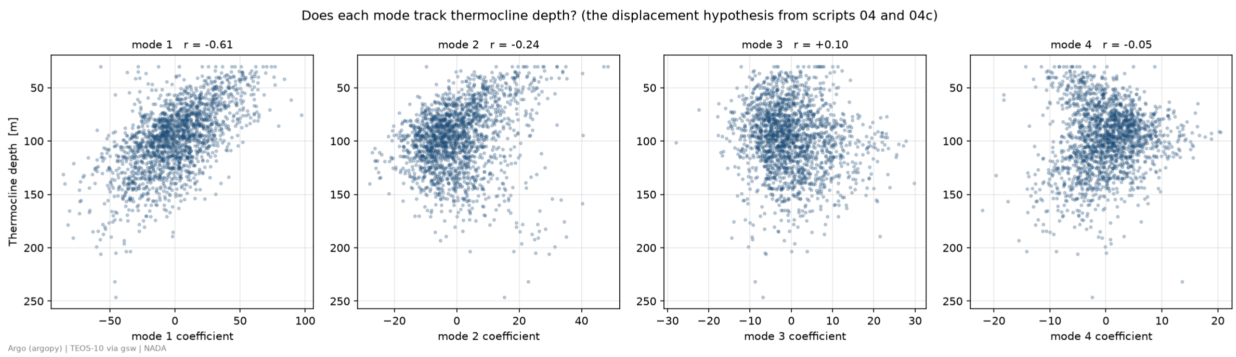

Figure 3: Mode coefficients against thermocline depth for the first four modes. Mode 1 tracks thermocline displacement ($r = -0.61$); the higher modes do not ($r = -0.24$, $+0.10$, -0.05).

Table 1: The two ceilings. Oracle uses exact coefficients; predicted uses the random forest on surface observables. Held-out set, $n = 1261$, 1500 Hz, source 30 m. Climatology classifies 76.3 % correctly at an RMS error of 3.981 m s^{-1}.

	Oracle (exact coefficients)		Predicted (from surface)	
K	RMS (m s^{-1})	duct correct (%)	RMS (m s^{-1})	duct correct (%)
4	0.906	75.3	2.124	77.1
6	0.644	81.0	2.101	78.3
8	0.491	87.2	2.095	78.5
12	0.333	91.6	2.092	78.3

answer, four times more accurate in the standard metric, is *worse* at the question the acoustics actually asks. Truncation error is not benign noise for a threshold quantity; it is structured, and being confidently almost-right can be worse than not trying. A related artifact - a spurious convergence zone generated by an over-steep reconstructed mixed-layer gradient - has been reported for single-EOF regression in the South China Sea [Chen et al.(2023)].

The missing structure is real and recoverable in principle. Going from four to twelve modes raises oracle classification from 75.3 to 91.6 %. Modes 5–12 carry only 4.4 % of the variance and 16.3 percentage points of duct accuracy. Variance ranking and acoustic relevance are close to orthogonal.

The surface cannot supply it. The predicted column is flat. Adding modes beyond $K = 6$ changes duct accuracy by less than half a point and RMS by 0.01 m s^{-1}. Mode-by-mode, perfect surface observables recover modes 1–4 at mean $R^2 = 0.409$ and modes 5–12 at mean $R^2 = 0.100$. The modes are not invisible - but their visibility converts to 1.2 percentage points of duct accuracy, leaving **13.3 percentage points** that exist in the profile, are representable in the basis, and are not obtainable from the surface. The predictors used here are noiseless and exactly collocated, so 78.3 % is an upper bound on any satellite-driven product in this basin.

Independent support comes from an older and quite different experiment: Jain and Ali [Jain et al.(2007)] estimated sonic layer depth from surface parameters in the Arabian Sea with a neural network and obtained an RMSE of about 11.8 m. Our SLD mean absolute error is 12.8 m to 13.3 m. Two methods, two basins, nineteen years apart, the same wall.

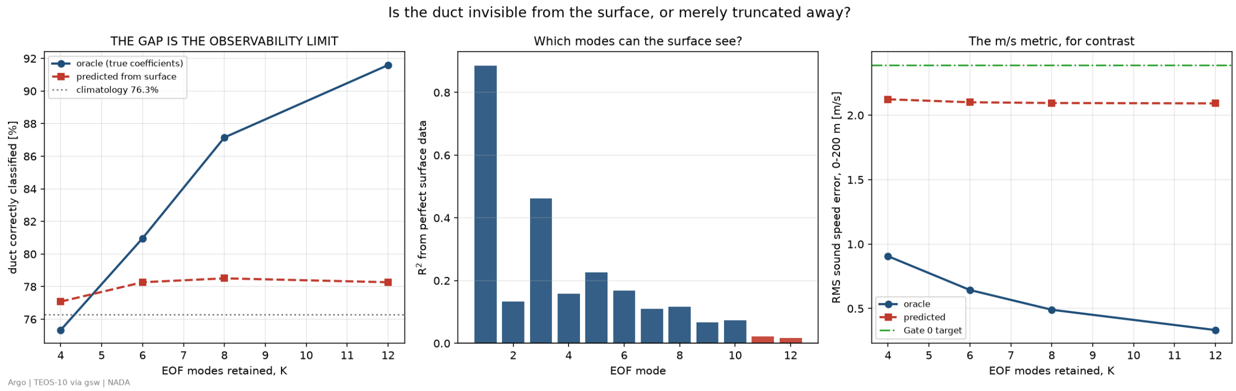

Figure 4: The two ceilings. Left: duct classification against truncation order for the oracle (exact coefficients) and for prediction from perfect surface observables; the gap between them is the observability limit. Centre: coefficient R^2 by mode. Right: the RMS metric, for contrast.

4.4 Coupling between profile error and acoustic error

Figure 5 and Table 2 give the coupling between profile RMS error and acoustic error at 10 km.

Across 81 climatology runs at three frequencies, sound speed RMS error correlates with the *signed* over-prediction of range at $r = +0.548$, and with the *magnitude* of the error at only $r = +0.346$. These are different claims and the distinction has been blurred in previous informal statements of this result: RMSE explains 30 % of the variance in how far climatology over-promises, but only 12 % of the variance in how wrong it is.

Both figures are moreover *upper bounds*, because the 81-run sample deliberately appended the three largest RMS errors in the candidate pool. Selecting cases on the x variable and then correlating with x stretches the range and inflates r. On the stratified 24-location sample without worst-case augmentation the correlations are weaker throughout, and within the estimator population they vanish: $r = +0.028$ for the RMSE-trained estimator and $r = -0.171$ for the duct-weighted one.

Table 2: Profile error against acoustic error, energy metric at 10 km, 24 locations × 3 frequencies ($n = 66$ per variant). Sound speed errors here are means of per-location RMS and are *not* the pooled held-out values quoted elsewhere.

	mean RMS ($\mathrm{m\,s^{-1}}$)	mean $\lvert\Delta\mathrm{TL}\rvert$ (dB)	r (signed)	r ($\lvert$error$\rvert$)
Climatology	3.948	13.77	+0.363	−0.039
Estimator, m/s loss	1.784	11.64	+0.028	−0.128
Estimator, duct loss	1.687	15.00	−0.171	+0.098

The inversion is visible in the table. The variant with the *smallest* profile error has the *largest* acoustic error.

Decomposing by regime explains why. When a variant and the ocean agree that the source is trapped, the RMSE-trained estimator achieves 4.9 dB ($n = 29$), 15.0 dB when they agree the source is not trapped ($n = 25$), and 21.0 dB when they disagree ($n = 12$). The spread across regimes, a factor of 4.3, exceeds the spread across methods within a regime. Regime is the dominant term. Disagreement rates are 14, 18 and 20 % for climatology and the two estimators respectively - differences of three to four cases out of 66, which we do not interpret. The better powered comparison over 1261 profiles gives 76.3, 77.1 and 78.6 %: no method is meaningfully better at the duct.

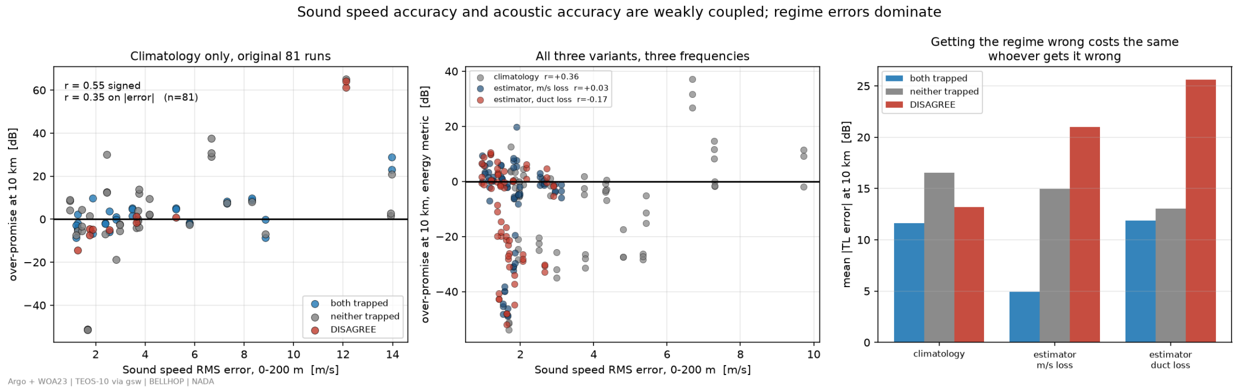

Figure 5: Profile error against acoustic error. Left: climatology only, original 81 runs (80 of 81 runs return a value at 10 km), coloured by whether climatology and the ocean agree about trapping. Centre: all three variants at three frequencies. Right: mean absolute TL error decomposed by regime agreement.

4.5 A pre-registered intervention

Correlational evidence cannot establish that optimising the standard metric fails to buy acoustic skill. We therefore intervened. A second estimator was trained with a depth-weighted objective, $w(z) = 1 + 3\exp[-(z/60)^2]$, emphasising the duct region. The following criterion was fixed in writing before any acoustic result was computed:

> *The duct-weighted estimator must beat the RMSE-trained estimator by at least 1.5 dB in mean absolute transmission loss error, or this is a negative result. No extension, no tuning, no third variant.*

The weighting did what it was designed to do in profile space: RMS error over 0 m to 200 m fell from 2.124 to 2.086 $\mathrm{m\,s^{-1}}$, over 0 m to 80 m from 1.878 to 1.762 $\mathrm{m\,s^{-1}}$, and duct classification rose from 77.1 to 78.6 %.

It did not convert. At 10 km over 22 paired locations the improvement was −3.97 dB with a 95 % bootstrap interval of $[-9.24, +0.86]$ (Figure 6). The criterion is not met, and because the upper bound of the interval lies below 1.5 dB, the pre-registered effect is excluded at 95 % confidence.

We are careful about what this does *not* show. The interval covers zero; the paired difference is positive at 11 of 22 locations; the three largest differences supply 95 % of the mean; and a paired Wilcoxon test gives $p = 0.337$. The two estimators are not distinguishable on this metric at this sample size. The claim is that duct weighting did not improve acoustic prediction by the pre-registered margin, not that it made it worse.

4.6 Real altimetry

The height predictor used above is dynamic height computed from each profile's own temperature and salinity. No instrument delivers that; it is a ceiling. Table 3 and Figure 7 give the cost of replacing it with DUACS altimetry.

Three observations. First, altimetry does all the work: removing the height term entirely drives mode-1 R^2 to −0.187, worse than predicting the seasonal mean, and duct accuracy below

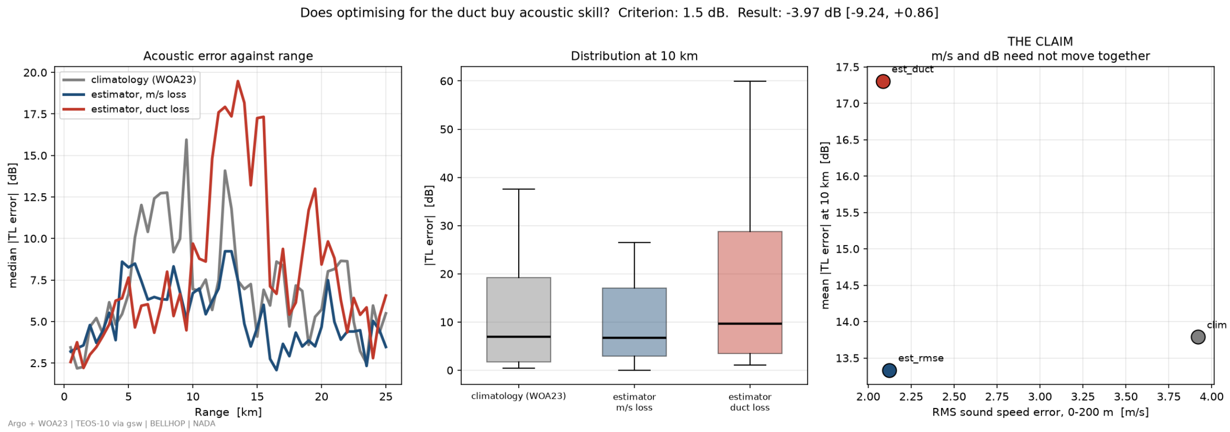

Figure 6: The pre-registered intervention. Left: median absolute TL error against range. Centre: distribution at 10 km. Right: mean absolute TL error against sound speed RMS error for the three variants; the two axes do not order the methods the same way.

Table 3: Cost of using a real instrument. Pooled over 1261 held-out profiles, season-stratified $K = 4$ basis, random forest.

Height predictor	RMS ($\mathrm{m\,s^{-1}}$)	mode-1 R^2	duct correct (%)
none	4.259	−0.187	70.8
dynamic height (idealised)	2.124	+0.883	77.1
`sla` (satellite)	3.016	+0.570	76.7
`adt` (satellite)	2.928	+0.599	75.8
`sla` + `adt`	2.923	+0.603	76.2

climatology's. Second, the real instrument costs $0.80\,\mathrm{m\,s^{-1}}$, moving the estimator from inside a nominal $2.389\,\mathrm{m\,s^{-1}}$ accuracy target to 1.22 times over it. Third, and most relevant to this paper, that $0.80\,\mathrm{m\,s^{-1}}$ degradation changes duct classification by 0.9 percentage points. **A quarter of the profile accuracy is lost and the acoustically decisive quantity does not move.**

The mechanism is a mismatch of definition compounded by basin physics. Our idealised term is dynamic height over 0 m to 480 m; altimetry senses the full column's steric signal plus a mass component. In the Bay of Bengal a substantial part of the seasonal sea level signal is halosteric - the freshwater cap expanding the column - rather than thermosteric thermocline displacement. The river that makes the acoustics difficult also contaminates the one surface observable that was working. Quantitatively, after removing position and season the two quantities correlate at $r = 0.871$ (`sla`) and $r = 0.904$ (`adt`), so roughly a quarter of the variance in the idealised predictor is not seen by the instrument, and mode-1 skill falls from 0.883 to 0.570–0.603 accordingly.

4.7 Frequency robustness

The results above were obtained at 1500 Hz. Table 4 repeats the comparison at 500 and 3500 Hz over the same 24 locations and the same profiles.

On the energy metric the ordering is identical at all three frequencies, and the inversion replicates: the variant with the lowest profile RMS error has the highest acoustic error at every frequency. Reducing profile RMS error by 47 % relative to climatology buys only a 12 % to 17 % reduction in acoustic error at 500, 1500 and 3500 Hz - an exchange rate near 0.3, stable across the sweep. The

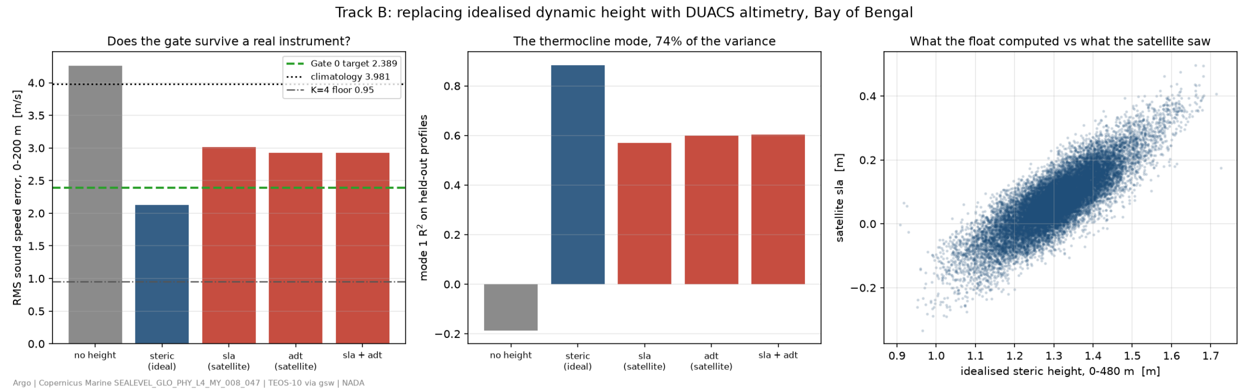

Figure 7: Replacing idealised dynamic height with DUACS altimetry. Left: RMS sound speed error by predictor set. Centre: mode-1 R^2. Right: idealised dynamic height against satellite sea level anomaly for all 19 934 collocated profiles.

Table 4: Mean absolute TL error at 10 km across a factor of seven in frequency. Energy metric is primary; point-wise shown for comparison. Of the 24 locations, 20 to 22 returned a value for every variant at the 10 km bin.

Frequency	Metric	Climatology (dB)	Estimator, m/s (dB)	Estimator, duct (dB)
500 Hz	point	14.85	17.32	16.49
	energy	12.77	11.18	15.03
1500 Hz	point	15.73	14.24	18.07
	energy	13.90	11.64	14.74
3500 Hz	point	13.98	16.41	19.04
	energy	14.64	12.10	15.25

duct-weighted estimator fails the 1.5 dB bar in all nine frequency–metric combinations.

The point-wise metric, by contrast, ranks the estimator worse than climatology at 500 and 3500 Hz, which is the empirical basis for the choice of primary metric in Section 3.4.

5 Discussion

5.1 What this implies for evaluation

The practical recommendation is narrow and, we think, hard to argue with: *an SSP product intended for acoustic use should be reported with an acoustic metric alongside its profile metric.* That is inexpensive. BELLHOP over a few tens of profiles costs minutes. Several recent studies already do this [Li et al.(2024), Yang et al.(2026)]; we suggest it become the norm rather than a supplementary check, and that the acoustic metric be an energy-averaged one for the reasons in Section 3.4.

A second recommendation concerns truncation. The order K is almost always chosen by cumulative variance or reconstruction RMSE. For acoustic applications this selects for the wrong thing. If a regime-sensitive criterion - duct classification accuracy against exact-coefficient reconstruction - were used instead, the selected order in this basin would be at least 8 rather than 4. That such a

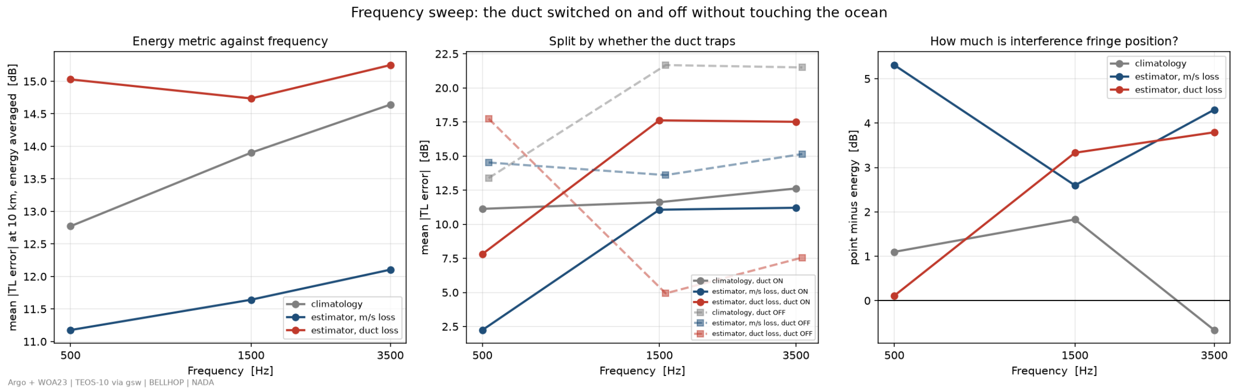

Figure 8: Frequency sweep over the same 24 locations. Left: energy metric against frequency. Centre: split by whether the duct traps at each frequency, per Eq. (1). Right: difference between point-wise and energy-averaged error, which widens with frequency as Eq. (2) predicts.

basis cannot be driven from the surface is a separate problem, and an informative one. Sparse and learned bases - compressive sensing over normal modes or dictionaries [Bianco and Gerstoft(2016)] - are one route to representing near-surface structure with fewer coefficients, and are worth testing against a regime-sensitive criterion rather than an RMSE one.

5.2 Why the coupling is weak

Two mechanisms, of different kinds, act together.

The first is categorical. Duct trapping is a threshold condition (Eq. 1); a profile is either on one side of it or the other. When a method and the ocean agree that the source is trapped, error is 4.9 dB to 11.9 dB; when they agree it is not trapped, 13.1 dB to 16.5 dB; when they disagree, 13.2 dB to 25.6 dB. For both estimators disagreement is the most expensive case by a wide margin (21.0 and 25.6 dB); for climatology it is not, which we attribute to climatology being smooth enough that its near-misses are mild. A metric that averages sound speed error over the column cannot see a threshold. This is recognised operationally: U.S. Navy work on modifying synthetic profiles to correct the mixed layer depth is motivated explicitly by the resulting transmission loss error [Barron and Helber(2011)].

The second is a coherence limit (Eq. 2). At the frequencies and ranges considered, prediction of the coherent field would require sound speed accuracy one to two orders of magnitude beyond what any surface-driven estimator, or even the truncation floor of the basis, can deliver. Only energetic quantities are predictable, and only statistically. This is the same physical constraint that underlies the travel-time resolution requirements of ocean acoustic tomography [Munk and Wunsch(1979)], approached from the opposite direction.

5.3 Limitations

The acoustic sample is 24 locations in one geometry - a 200 m shelf, a single seabed model, source and receiver both at 30 m. The tail of the TL error distribution is heavy, so means are unstable at this sample size and we have reported medians and intervals alongside them throughout. Subgroup splits with $n < 15$ are reported for completeness and are not interpreted.

Sea surface temperature and salinity are taken from the float rather than from satellites. Their contribution is small - together they account for $0.105\,\mathrm{m\,s^{-1}}$ of a $2.135\,\mathrm{m\,s^{-1}}$ effect - but the reported satellite performance is therefore an upper bound. Satellite salinity in this basin is additionally degraded by radio-frequency interference and the freshwater plume.

The altimetry is a gridded L4 product with a ±6 week mapping window and correlation scales exceeding 100 km. Along-track L3 data close in time to each float may retain more information. The correct statement of Section 4.6 is therefore that *gridded* altimetry does not reach the required accuracy.

Finally, the basin's sea level signal contains a large halosteric component. Estimating and removing it, using satellite salinity and ocean bottom pressure from gravimetry, is the natural next experiment and is not attempted here.

6 Conclusions

Sound speed profile RMS error and acoustic prediction error are weakly coupled in the Bay of Bengal, and across the three methods examined here they are inverted: the method with the smallest profile error has the largest acoustic error, at all three frequencies tested.

The mechanism is a property of the basis rather than of any estimator. A variance-ranked EOF expansion places its leading modes at the depth of maximum variance, near 100 m, while surface-duct trapping is decided in the upper 60 m. Given exact coefficients, four modes classify the propagation regime less accurately than climatology despite an RMS error 4.4 times smaller; twelve modes classify it well. The missing modes carry 4.4 % of the variance and 16.3 percentage points of duct accuracy.

Those modes are recovered from perfect surface observables at mean $R^2 = 0.10$, leaving a 13.3 percentage-point gap between what the profile contains and what the surface can supply. Real gridded altimetry degrades profile accuracy by $0.80\,\mathrm{m\,s^{-1}}$ while leaving duct classification unchanged within one percentage point.

Two conclusions follow. Products intended for acoustic use should be evaluated acoustically, with an energy-averaged metric and a regime-sensitive truncation criterion. And in this basin, the accuracy the acoustics requires is not available from the surface at any objective weighting, which is an argument for measuring the acoustic field directly.

Data and code availability

All data are public. Argo profiles are from the International Argo Program; World Ocean Atlas 2023 from NOAA NCEI; sea level from the Copernicus Marine Service product `SEALEVEL_GLO_PHY_L4_MY_008_047`. Analysis code, derived data products, and a provenance ledger recording the source, population and aggregation of every number in this paper are archived at `https://doi.org/10.5281/zenodo.22802582` and developed at `https://github.com/deringeorge-nebula/nada-bob-ssp`.

Acknowledgements

Figures carry the provenance label NADA, the internal designation of this research programme at Thalwag. Argo data were collected and made freely available by the International Argo Program and the national programmes that contribute to it (doi: 10.17882/42182). This study has been conducted using E.U. Copernicus Marine Service Information.

Competing interests

The author is affiliated with Thalwag, which conducts research on ocean acoustic observation. This work received no funding, describes no commercial product, and the analysis code and provenance ledger are published in full so that every number can be independently recomputed.

Funding

None.

References

[Carnes et al.(1990)] Carnes, M. R., Mitchell, J. L., and de Witt, P. W. (1990). Synthetic temperature profiles derived from Geosat altimetry: comparison with air-dropped expendable bathythermograph profiles. *Journal of Geophysical Research: Oceans*, 95(C10), 17979–17992. doi: 10.1029/JC095iC10p17979

[Fox et al.(2002)] Fox, D. N., Barron, C. N., Carnes, M. R., Booda, M., Peggion, G., and Van Gurley, R. (2002). The Modular Ocean Data Assimilation System (MODAS). *Oceanography*, 15(1), 22–28. doi: 10.5670/oceanog.2002.32

[Jain et al.(2007)] Jain, S., Ali, M. M., and Sen, P. N. (2007). Estimation of sonic layer depth from surface parameters. *Geophysical Research Letters*, 34(17), L17602. doi: 10.1029/2007GL030577

[Bianco and Gerstoft(2016)] Bianco, M. J., and Gerstoft, P. (2016). Compressive acoustic sound speed profile estimation. *The Journal of the Acoustical Society of America*, 139(3), EL90–EL94. doi: 10.1121/1.4943784

[Ou et al.(2022)] Ou, Z., Qu, K., Shi, M., Wang, Y., and Zhou, J. (2022). Estimation of sound speed profiles based on remote sensing parameters using a scalable end-to-end tree boosting model. *Frontiers in Marine Science*, 9, 1051820. doi: 10.3389/fmars.2022.1051820

[Li et al.(2024)] Li, P., Dong, C., et al. (2024). Reconstructing the sound speed profile of the South China Sea using remote sensing data and long short-term memory neural networks. *Frontiers in Marine Science*, 11, 1375766. doi: 10.3389/fmars.2024.1375766

[Li et al.(2025)] Li, H., Liu, Y., Wang, P., Li, M., Zhu, Y., Mao, K., and Chen, X. (2025). A deep learning-based reconstruction model for 3D sound speed fields combining underwater vertical information. *Frontiers in Marine Science*, 12, 1551823. doi: 10.3389/fmars.2025.1551823

[Yang et al.(2026)] Yang, J., Xie, D., Chen, C., and Wen, J. (2026). Full-depth dynamic gradient-guided residual correction for daily three-dimensional ocean sound speed prediction. *Sensors*, 26(15), 4939. doi: 10.3390/s26154939

[Chen et al.(2023)] Chen, Z., et al. (2023). Reconstruction of the sound speed profile in typical sea areas based on the single empirical orthogonal function regression method. *Journal of Marine Science and Engineering*, 11(4), 841. doi: 10.3390/jmse11040841

[Munk and Wunsch(1979)] Munk, W., and Wunsch, C. (1979). Ocean acoustic tomography: a scheme for large scale monitoring. *Deep-Sea Research Part A*, 26(2), 123–161. doi: 10.1016/0198-0149(79)90073-6

[Barron and Helber(2011)] Barron, C. N., and Helber, R. W. (2011). MLD-modified synthetic ocean profiles. U.S. Patent 8,032,314, granted October 4, 2011; Assignee: The United States of America as represented by the Secretary of the Navy.